Research Activities in the Frame of the S3 Project

Emolo A.[1], Caccavale M.[1], Convertito V.[2], Delouis B.[3], De Matteis R.[4], Di Crosta M.[1,6], Festa G.[1]
Gallovic F.[1,5], Lucca E.[1], Satriano C.[1,6], Stabile T.A.[1,6], Zahradnik J.[5], Zollo A.[1]

amra analysis and monitoring of environmental risk

(1) Dept. of Physics, University "Federico II", Naples, Italy, antonio.emolo@na.infn.it, (2) INGV – Osservatorio Vesuviano, Naples, Italy, converti@na.infn.it (3) Géosciences Azur, University of Nice, Sophia Antipolis, France, delouis@geoazur.unice.fr, (4) DSGA, Sannio University, Benevento, Italy, dematteis@unisannio.it, (5) Dept. of Geophysics, Charles University, Prague, Czech Republic, jz@karel.troja.mff.cuni.cz (6) AMRA scarl, Naples, Italy

Università degli Studi del Sannio

INGV

GeoAzur TERRE - OCÉAN - ESPACE

The DSF-UniNA research unit has performed activities concerning the moment tensor estimation, the ground motion simulation, the kinematic source inversion, and the determination of ground motion predictive equations.

The moment tensor solution is determined by modelling the strong-motion waveforms using two different approaches. The former one uses the point source approximation and performs a grid search over a set of trial source positions and time shifts in order to identify the optimal centroid position, time and moment tensor through a minimization of the residual errors. In the second method the rupture is represented by a finite 1D source model. Source finiteness is approximated by a summation over point sources aligned along fault strike. The focal mechanism and the linear seismic moment distribution along the strike of the fault are inverted at the same time using a fast and optimized grid search combined with a simulated annealing algorithm.

Concerning the seismic wavefield simulation, it is numerically modeled using three different algorithms. The first, based on the asymptotic ray-theory approximation, rapidly computes high frequency seismograms including direct and reflected waves from 1D velocity models.

The second code uses an hybrid approach, with the low frequency seismograms computed by a discrete wave number method and enriched by stochastic high frequency modeling. Finally, a high-order spectral element method code is used for the full 3D numerical modeling of the wavefield.

The kinematic inversion is aimed at determining the rupture direction, the final slip distribution on the fault plane and the propagation velocity of the rupture. The methodology is based on representation integral, in the form proposed by Burridge and Knopoff (1964). It is solved by a finite elements technique that uses a Delaunay's fault plane triangulation. The slip is parameterized through a 2D Gaussian overlapping functions, and the inverse problem is solved using the Neighbourhood algorithm with a L2 norm.

Finally, we estimated a GMPE for low-magnitude earthquakes (M< 4.0) in the Campania-Lucania region in southern Apennines (Italy. The model concerned peak ground acceleration (PGA) and velocity (PGV) and has been retrieved on a data-set of about 160 earthquakes recorded by the Irpinia Seismic Network (ISNet) (Iannaccone et al., 2009) in the last four years.

Simulations

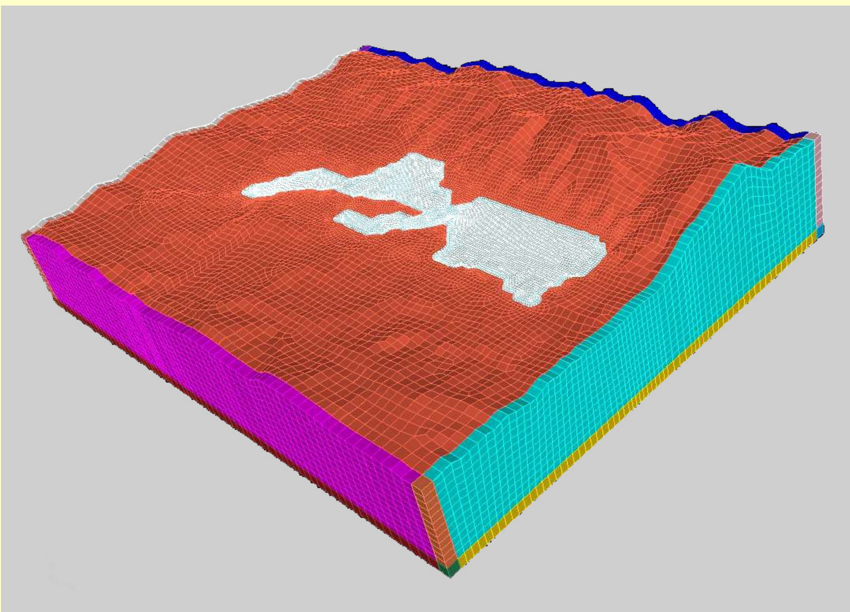

3D Spectral Element Method

We will investigate the wave propagation in the L'Aquila basin with the 3D Spectral Element Method (SEM) Parallel Code– 3DSPEC (Festa and Vilotte, 2006; Delavaud et al., 2006). SEM is very efficient in solving the complete wavefield, within complex sources, by combining the accuracy of spectral methods and the flexibility in the meshing, typical of finite-element codes. SEM approximates the solution with piecewise high-order Lagrange polynomials, localized at the Gauss-Lobatto-Legendre quadrature points. Such a choice leads to a diagonal mass matrix and an explicit time-stepping scheme. The method efficiently accounts for topography, free-surface, complex basin shapes, velocity contrasts and absorbing boundary conditions, which mostly accounts for energy to quit the model at external boundaries. Rupture is kinematically imposed as a combination of point-sources opportunely activated when they are reached by the rupture front.

Multiphase Ray Theory Method

We will perform a fast computation of synthetic seismograms associated to an extended fault, considering a complex source kinematic model for the earthquake rupture process.

The source parametrization is based on k-square model (Herrero and Bernard, 1994; Gallovič and Brokešová, 2004).

The source is discretized by a grid of NxM point souces and the synthetic seismogram at each receiver, associated to the extended fault, is the sum of the synthetics computed for each point source.

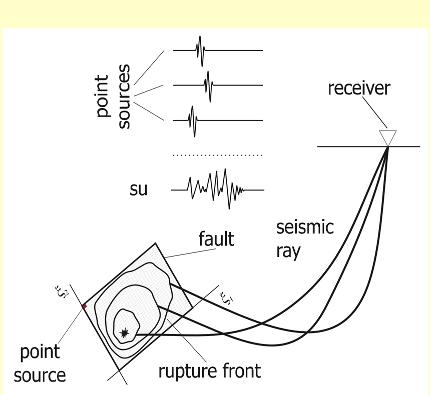

The computation of synthetic seismograms for each source is based on the asymptotic ray-theory. The method we developed allows the rapid generation of an exhaustive number of seismic-phases that are used to build seismic waveforms having the same complexity of records simulated by complete wave-field techniques.

The method uses a hierarchical order of ray and seismic-phase generation, taking into account existing constraints for ray paths and a number of physical constraints (Stabile et al., 2009). The algorithm has been implemented in the COMRAD code (from the Italian: "COdice Multifase per il RAy-tracing Dinamico").

Below an example of synthetic seismograms (X and Z component) computed in a layered velocity model for a station at 30 km epicentral distance from an explosive source (4 km depth) is shown. Each seismic phase can be indentified on waveforms.

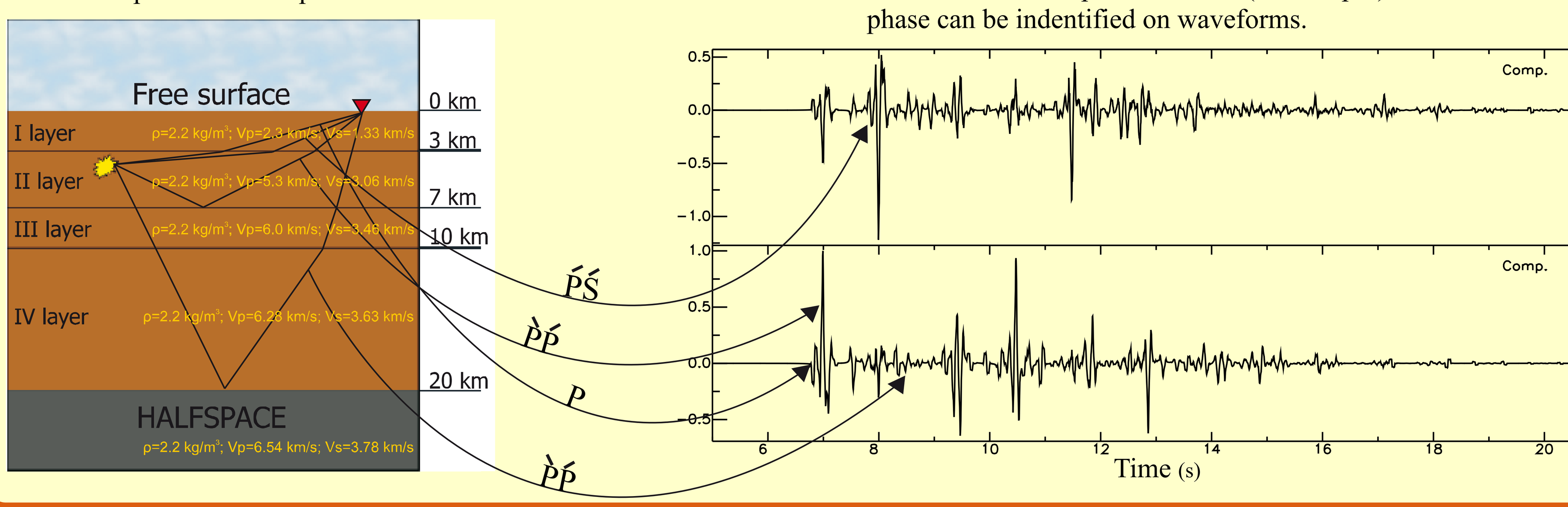

Moment tensor

The moment tensor solution for the L'Aquila main-shock has been determined by modelling the both the broad-band and strong-motion waveforms recorded at the ISNet network using two different approaches. The former (ISOLA, Sokos and Zahradnik, 2008) uses the point-source approximation and performs a grid search over a set of trial source positions and time shifts in order to identify the optimal centroid position, time and moment tensor through a minimization of the residual errors that is equivalent to maximize the correlation between real and synthetic seismograms.

In the second method (FMNEAREG, B. Delouis) the rupture is represented by a finite 1D source model. Source finiteness is approximated by a summation over point sources aligned along fault strike. The focal mechanism and the linear seismic moment distribution along the strike of the fault are inverted at the same time using a fast and optimized grid search combined with a simulated annealing algorithm.

We find a centroid depth of about 5 km and a prevalently normal fault plane solution with a dominant directivity effect toward SE.

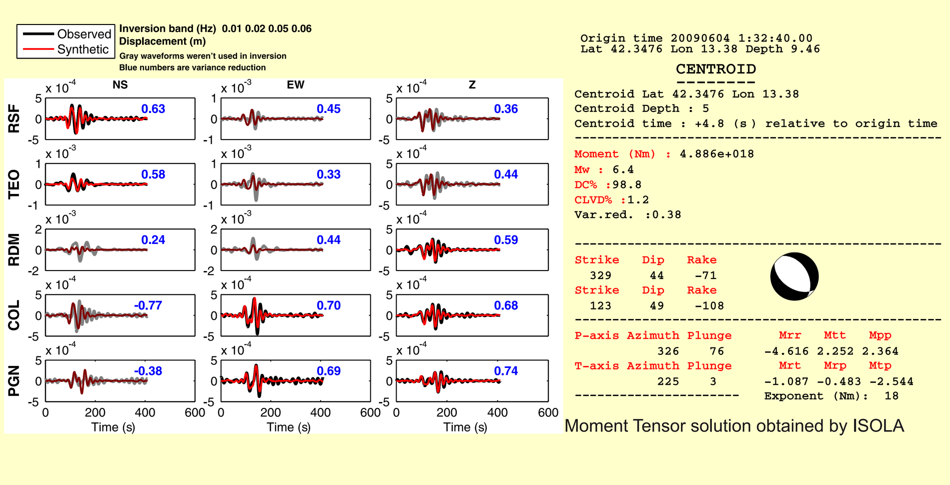

Moment Tensor Solution obtained by ISOLA

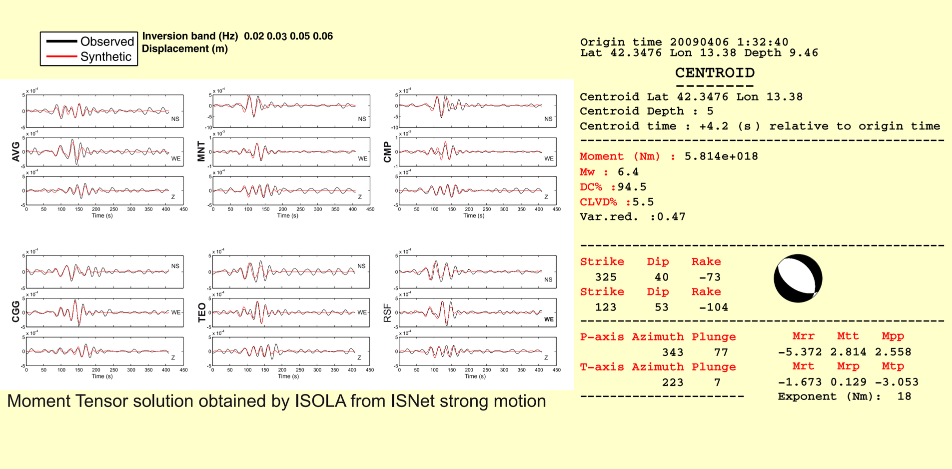

Moment Tensor Solution obtained by ISOLA from ISNet strong motion

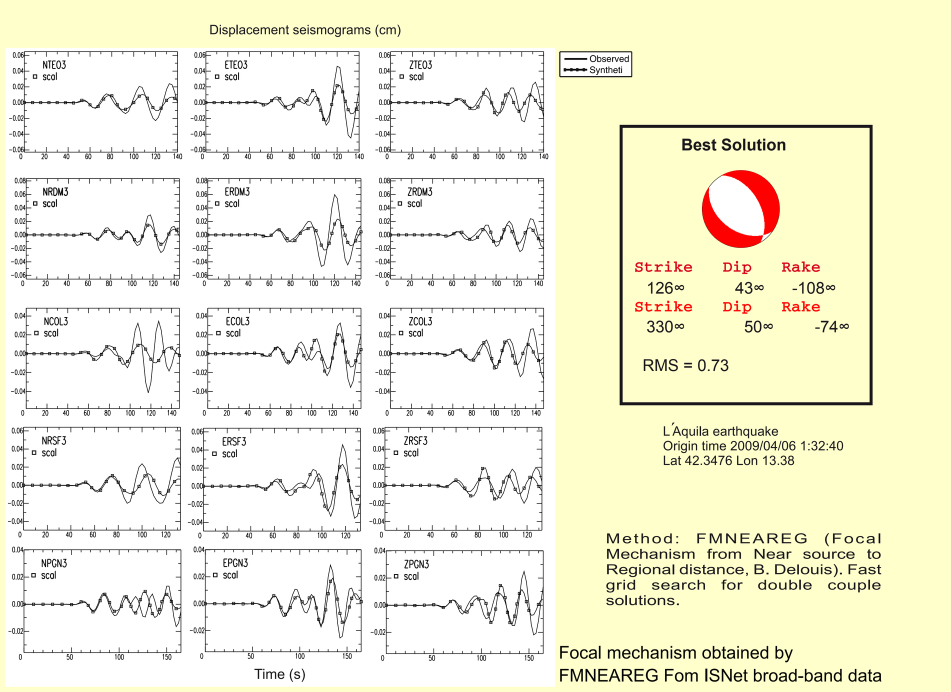

Focal mechanism obtained by FMNEAREG Fom ISNet broad-band data

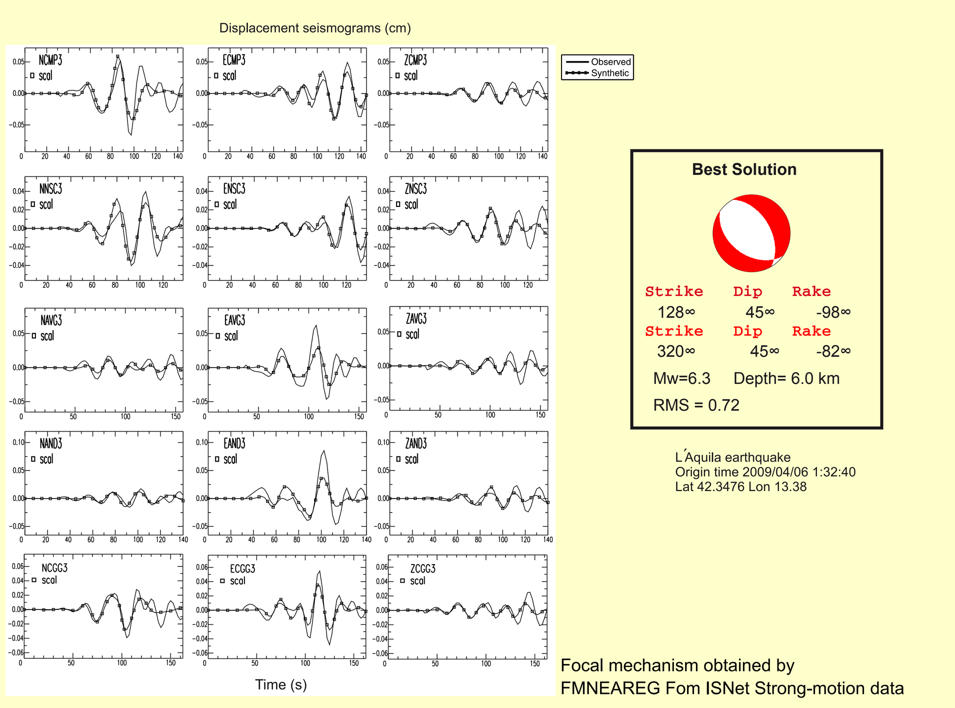

Focal mechanism obtained by FMNEAREG Fom ISNet Strong-motion data

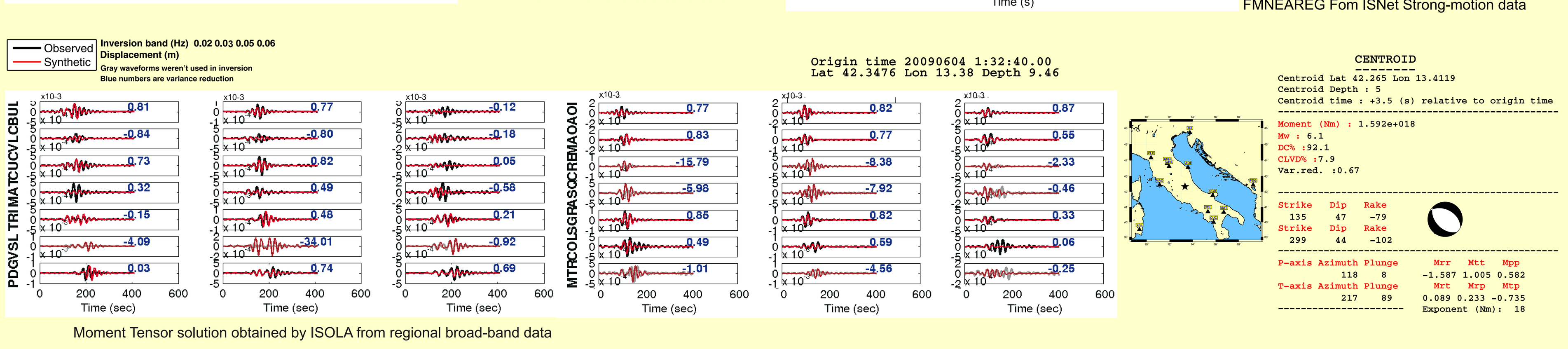

Moment Tensor Solution obtained by ISOLA from regional broad-band data

Kinematic inversion

Slip and rupture velocity distribution are inverted along the fault plane. The forward problem is based on the solution of the representation integral in the frequency domain, solved by a finite element approach based on Delaunay's fault plane triangulation, over which the Green' tractions are computed. A different parametrization for slip and rupture velocity is chosen : the slip is described by 2D overlapping Gaussian functions, the rupture speed by cells with constant values. The inverse problem is solved as an optimization problem, using the Neighbourhood algorithm with a L2 norm. The methodology has been applied to a 2008, June 14, Iwate-Nairiku-Miyagi, Japan, earthquake (M = 7.2), recorded by K-net and Kik-net stations.

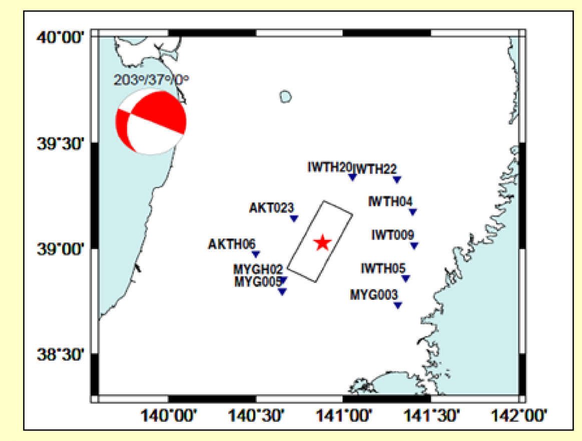

Geometry source-receiver. The strong motion accelerograms were used in inversion, and were recorded from the ten station shows in the map.

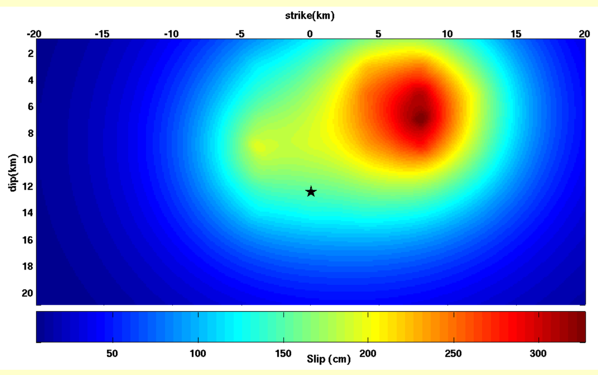

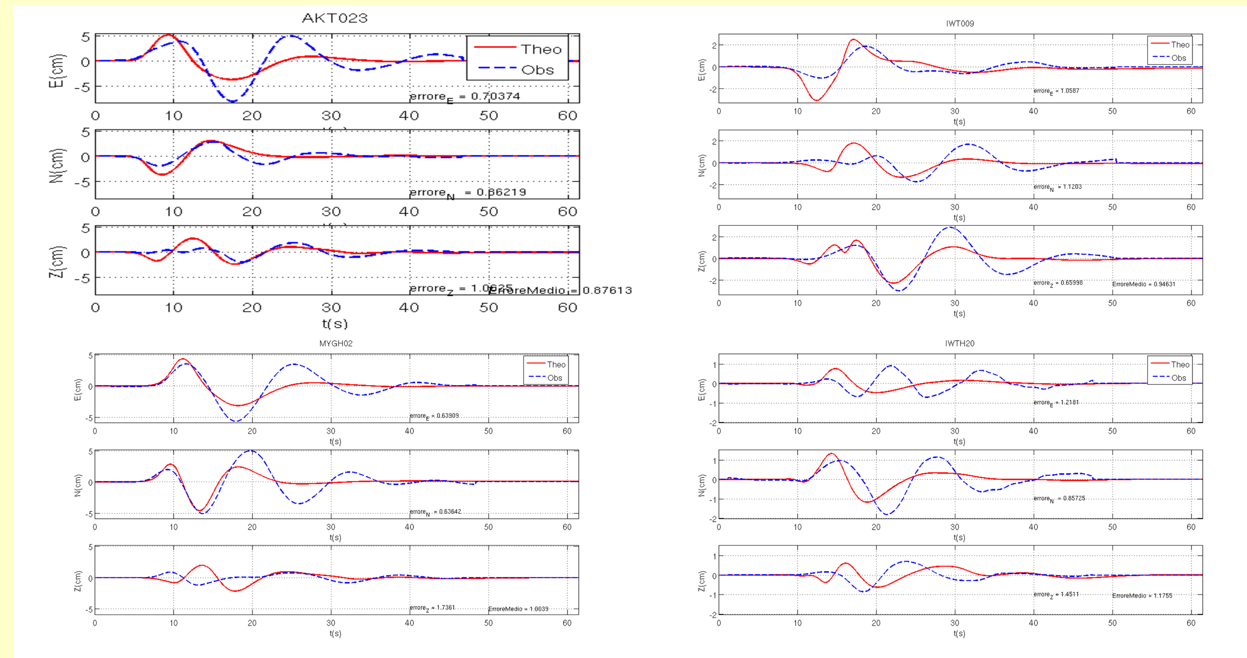

Matching data with synthetics. The waveforms, plotted in blue, are compared with synthetic seismograms (red line) for four selected station: AKT023, IWT009, MYGH02, IWTH20.

Figure shows the resultant slip distribution to the inversion, on the NW dipping fault plane, where slips are drawn in a color scale. The black star denotes the hypocenter. The rupture velocity and moment magnitude are estimated to be 2.8 km/s and 6.8, respectively. The estimated slip distribution is similar to that inversion of Hikima K., 2008.

Ground-motion prediction equations for low-to-moderate earthquakes in the Campania-Lucania region, Southern Apennines, Italy

A key aspect of ground-shaking map calculation is represented by ground motion prediction equations. In fact, ground-shaking maps soon after an earthquake, are calculated by integrating observed data and estimates for the areas not covered by seismic network (Wald et al., 1999; Convertito et al., 2009).

Nowadays' empirical ground motion models used to compute ground shaking maps primarily refer to strong ground motion due to large earthquakes (M > 5.5). However, those models cannot be properly used to predict ground motion due to small magnitude earthquakes which, due to their frequency of occurrence, and highest frequency content can affect non-structural component of both industrial facilities and civil structures.

Ground-motion prediction equations (GMPEs) for peak-ground acceleration and peak-ground velocity are presented in this study. The dataset used is relative to the seismicity recorded by the Irpinia Seismic Netwrok (ISNet) in the last years (Iannaccone et al., 2009).

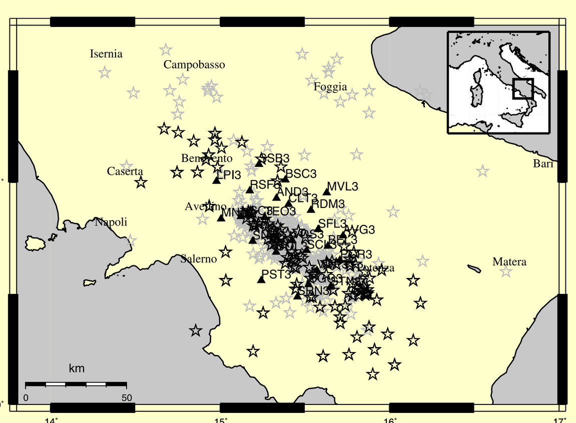

Figure 1: Recent seismicity (grey stars) recorded at ISNet and the earthquakes selected for the aim of the present study (black stars) included in the area delimited by the dashed lines. Largest part of the recorded seismicity is located along the Apenninic belt chain in the area containing the seismogenic structure where the last destructive MS 6.9 23 November 1980

Because the retrieved models are used for ground-shaking map calculation in the Campania-Lucania region, Southern Apennines, Italy, they refer to rock-sites. In fact, site effect is accounted for by using both a geological map and corrective coefficients for the main geological formation in outcrop in the area of interest.

A two steps procedure has been applied to retrieve the GMPEs. First, a reference GMPE for rock-site is retrieved. Next, in order to discriminate stations affected by station-effects, the residuals' distribution have been calculated. The GMPEs are then modified to take into account for the station-effect.

Ground-motion prediction equations for Pga and Pgv

The data reduced to rock site, by using the QVTM map and associated corrective coefficients provided by Cantore (2008), have been first used to retrieve a reference model and then have been used to calculate the residuals' distribution at each single station in order to identify station effect. To this aim, once the best reference model has been retrieved, at each station the distribution of the residuals is considered and its mean value is tested against the null hypothesis of being zero at 5% significance level through a Z-test (critical value zc=±1.96). Once all the stations have been tested and identified as affected or not by station effect, a new GMPE with an additional parameter has been retrieved. Panels a and b of Figure 2 show the residuals distribution Pga and Pgv respectively.

Corrected ground-motion model

Once each station has been classified following the procedure described in the previous section, a station-dependent model has been considered by adding an additional coefficient in the model which ah the following formulation:

$$LogY = a + bM + c\log R + ds \pm \sigma_{\log Y}$$

	a	*b*	*c*	*d*	σ_{logPGX}
Pga (m/s^2)	-1.817	0.460	-1.428	0.271	0.417
Pgv (m/s)	-3.673	0.543	-1.463	0.120	0.347

Table 1: Regression coefficients of equation (5) and associated standard error for site dependent model.

Where M is magnitude, R is the hypocentral distance expressed in km, s is a dummy variable which assume values -1, 0 or 1 depending on the selected station (Figure 2) and σlogY is the standard error. The coefficients along with the standard error are listed in Table 1.

In order to the test the retrieved stations' dependent models, they have been compared with those proposed by Frisenda et al. (2005) (hereinafter FRI05) retrieved by using data relative to small earthquakes recorded in Northern Italy respectively and the ones proposed by Massa et al. (2007) (hereinafter MAS07) for Central-Northern Italy.

Figures 3 shows the results of the comparison for Pga and Pgv respectively. The GMPEs have been plotted by assuming the mean value of each magnitude class as reference magnitude and by considering both station effect for the model retrieved in the present paper and a no site-effect in the MAS07 model and FRI05 model. The analysis of the left panels of Figures 3 shows that the three models are characterized by different attenuation with distance. Those differences can be attributed both to a difference in tectonics of the region where data have been collected and to the limited number of data at small distances. Concerning Pgv, the differences are less marked and the three models are much more similar.

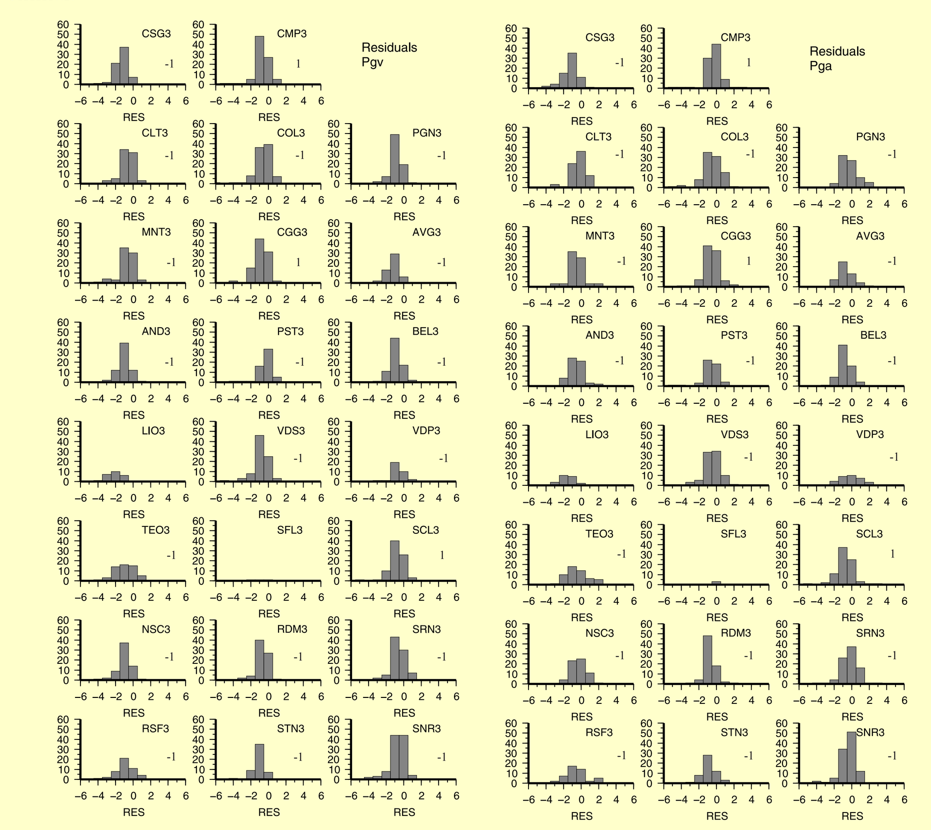

Figure 2: Residuals distribution for Pga and Pgv at each station of the INSet. On each plot, the number indicates if the station is not affected by station-effect (0), it is affected by positive station-effect (+1) or by negative stations-effect (-1).

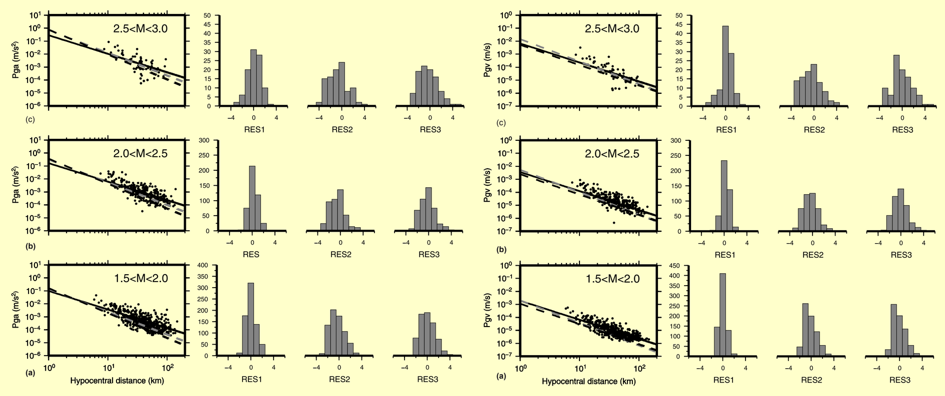

Figure 3: **Left:** Pga values and residuals' distribution for the three considered magnitude classes. Left panels show the Pga values as function of the hypocentral distance indicated as black points. On each panel, black lines indicate the GMPE retrieved in the present paper, while dashed line refers to MAS07 and grey line refers to FRI05. The corresponding residuals shown in the right panels are indicated as RES1, RES2 and RES3 respectively. **Right:** same as left but for Pgv.

Bibliography

Cantore L (2008) Determination of site amplification in the Campania-Lucania region (southern Italy) by comparison of different site-response estimation techniques. Ph.D. thesis, Dip. di Fisica, Universita` Federico II di Napoli

Convertito V., De Matteis R., Cantore L., Zollo A., Iannaccone G., Caccavale M. (2009). Rapid estimation of ground-shaking maps for seismic emergency management in the Campania Region of southern Italy. Nat Hazards. doi:10.1007/s11069-009-9359-2.

Frisenda M., M. Massa, D. Spallarossa, G. Ferretti and C. Eva (2005). Attenuation relationship for low magnitude earthquakes using standard seismometric records. J. Earthquake Eng. 9, 23-40.

Gallovič, F., Brokešová, J., 2004. On strong ground motion synthesis with k-2 slip distributions. Journal of Seismology 8, 211-224. doi:10.1023/B:JOSE.0000021438.79877.58.

Herrero, A., Bernard, P., 1994. A Kinematic Self-Similar Rupture Process for Earthquakes. Bulletin of the Seismological Society of America 84, 1216–1228.

Iannaccone G., Zollo A., Elia L., Convertito V., Satriano C., Martino C., Festa G., Lancieri M., Bobbio A., Stabile T. A., Vassallo and A. Emolo (2009). A prototype system for earthquake early-warning and alert management in southern Italy. Bulletin of Earthquake Engineering, doi: 10.1007/s10518-009-9131-8.

Stabile, T. A., De Matteis, R., Zollo, A., 2009. Method for rapid high-frequency seismogram calculation, Computers & Geosciences 35(2), 409-418. doi:10.1016/j.cageo.2008.02.030.

Sokos, E. and J. Zahradnik (2008). ISOLA: A Fortran code and a Matlab GUI to perform multiple-point source inversion of seismic data. Computers and Geosciences 34, 967-977.

Wald DJ, Quitoriano V, Heaton TH, Kanamori H, Scrivner CW, Worden CB. (1999) TriNet shakemaps: rapid generation of instrumental ground motion and intensity maps for earthquakes in southern California, Earthquake Spectra 15:537-555